

Photochromic Single-Component Organic Fulgide Ferroelectric with Photo-Triggered Polarization Response

Ye Du, Chao-Ran Huang, Zhe-Kun Xu, Wei Hu, Peng-Fei Li, Ren-Gen Xiong,* and Zhong-Xia Wang*



Cite This: *JACS Au* 2023, 3, 1464–1471



Read Online

ACCESS |

Metrics & More

Article Recommendations

Supporting Information

ABSTRACT: Organic photochromic compounds have been widely investigated for optical memory storage and switches. Very recently, we pioneeringly discovered optical control of ferroelectric polarization switching in organic photochromic salicylaldehyde Schiff base and diarylethene derivatives, differently from the traditional ferroelectrics. However, the study of such intriguing photo-triggered ferroelectrics is still in its infancy and relatively scarce. In this manuscript, we synthesized a pair of new organic single-component fulgide isomers, (*E* and *Z*)-3-(1-(4-(*tert*-butyl)phenyl)ethylidene)-4-(propan-2-ylidene)dihydrofuran-2,5-dione (1*E* and 1*Z*). They undergo prominent photochromism from yellow to red. Interestingly, only polar 1*E* has been proven to be ferroelectric, while the centrosymmetric 1*Z* does not meet the basic requirement for ferroelectricity. Besides, experimental evidence shows that the *Z*-form can be converted to the *E*-form by light irradiation. More importantly, the ferroelectric domains of 1*E* can be manipulated by light in the absence of an electric field, benefiting from the remarkable photoisomerization. 1*E* also adopts good fatigue resistance to the photocyclization reaction. As far as we know, this is the first example of organic fulgide ferroelectric reported with photo-triggered ferroelectric polarization response. This work has developed a new system for studying photo-triggered ferroelectrics and would also provide an expected perspective on developing ferroelectrics for optical applications in trap future.

KEYWORDS: organic ferroelectric, single-component, optical control, ferroelectric domain, fulgide



INTRODUCTION

Photochromism, a significant feature of light-responsive materials, has received excellent research attention for its neoteric application potentials such as optical switches and optical memory storage devices.^{1–10} It is remarkable that photochromic organic compounds possessing at least two isomeric forms upon light irradiation and superior natural merits including lightweight, low cost, easy processing, and so forth show growing demands in various application scenarios over a long period.

Ferroelectrics are a special class of polar crystalline materials, whose spontaneous electric polarization can be switched or reoriented under an external electric field. Such switchable polarization bistability allows ferroelectrics to be used as a key component in data storage applications.^{11–15} Since the first discovery of ferroelectricity in Rochelle salt,¹⁶ ferroelectrics have been extensively investigated and made considerable progress. In terms of the mechanism, traditional ferroelectrics undergoing paraelectric-ferroelectric phase transition are commonly stimulated by temperature, pressure, or magnetic field, which lead to the occurrence of displacive or ordered–disordered structural transition accompanying symmetry breaking in structures.^{17–28} Light as a non-contact, non-damaging remotely controlled media beyond the common

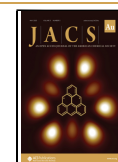
stimuli can also trigger structural changes.²⁹ Light-induced polarization response has been realized in several inorganic ferroelectrics.^{30–33} For example, optically excited lattice vibrations can actively induce the metastable polar ferroelectric phase in quantum paraelectric SrTiO₃.³³ Nevertheless, such an optical control of ferroelectricity does not involve intrinsic structural changes but relies on the secondary effects including light-driven stress, photon-excited electronic effects, and tuning complex interactions. Organic photochromic materials in the crystalline state show the reversible color change upon photoirradiation, generally arising from geometrical isomerization under specific wavelengths of light irradiation. Such light-induced structural isomerization can produce electronic as well as geometrical structure changes in the molecule, which may result in repositioning the orientation of the ferroelectric domains/polarization, under the premise of ensuring a polar point group in the crystal.¹⁸ Very recently, optical control of

Received: March 14, 2023

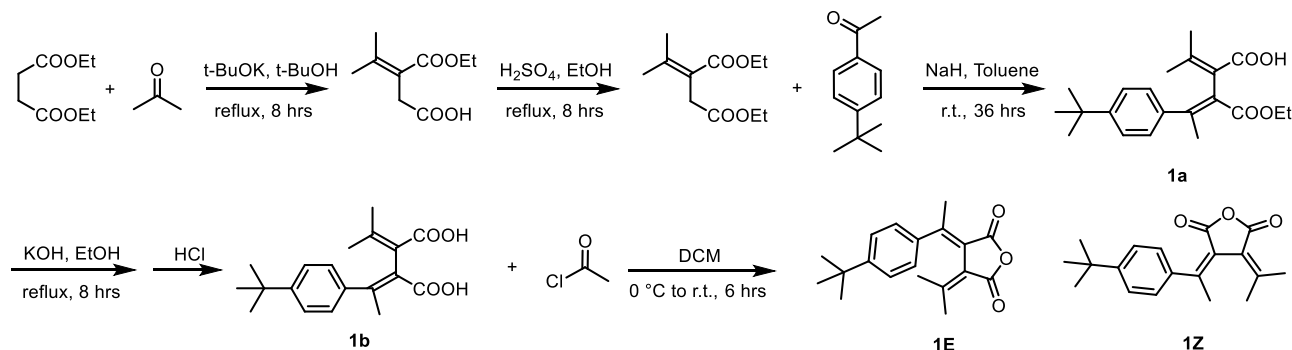
Revised: April 18, 2023

Accepted: April 19, 2023

Published: May 9, 2023



Scheme 1. Synthesis Procedure of Fulgides



polarization switching has been pioneeringly achieved in single-component photochromic organic ferroelectric salicylaldehyde Schiff base and diarylethene derivative crystals.^{34–38} Such optical manipulation of polarization is of milestone significance in the development of ferroelectrics. However, the study of such photo-triggered ferroelectric polarization response by photoisomerization is still in its infancy and relatively scarce.

Fulgides, which are derivatives of dimethylene-succinic anhydride, belong to one of the most important classes of photochromic compounds.³⁹ Since the first report by Stobbe more than a century ago, many studies toward fulgides have been carried out for hopeful applications in optical storage.^{39–51} Light irradiation of the fulgides generally undergoes a cyclization reaction to yield an excited cyclohexadiene derivative and reversely changes between the stable ring-opening and the unstable ring-closing forms. Although the spectroscopic and X-ray diffraction (XRD) studies on photochromism in fulgide crystals have been thoroughly investigated, their ferroelectricity and promising photo-triggered polarization response have never been documented so far.

In this work, we report two new organic photochromic fulgides (*E* and *Z*)-3-(1-(4-(*tert*-butyl)phenyl)ethylidene)-4-(propan-2-ylidene)dihydrofuran-2,5-dione (1E and 1Z), which are a pair of isomers. They undergo pericyclic photochemical reaction by light irradiation between the ring-opening form (pale-yellow) and the ring-closing form (deep-red). 1Z crystallizes in a centrosymmetric $P2_1/n$ space group, and 1E adopts a non-centrosymmetric structure (*Pc*). It is worth mentioning that the *Z*-form can be converted to the *E*-form by light irradiation, which has been confirmed by UV–vis spectra and time-dependent dynamic tracking of ^1H NMR. Significantly, the ferroelectricity of 1E was revealed by electric field-dependent polarization reversal. More strikingly, ferroelectric polarization of 1E detected by piezoresponse force microscopy (PFM) can be manipulated by light irradiation without an electric field. Besides, 1E shows good photoexcitation fatigue resistance during 20 switching cycles. Achieving intrinsic ferroelectricity and photo-triggered polarization response in the family of fulgides is rare. This work would provide great inspiration for the further development of photochromic ferroelectrics in optical applications.

RESULTS AND DISCUSSION

1E and 1Z were prepared by Stobbe condensations of diethyl isopropylidene succinate and *p*-*tert*-butylacetophenone (Scheme 1), the details of synthesis are described in the

Supporting Information.⁵² The pale-yellow crystals of 1E and 1Z were collected by slow evaporation of the as-synthesized power samples in the methanol solution, respectively. Their purity was verified by NMR and powder XRD (PXRD) spectra (Figures S1–S5). TGA results show that the stability of 1E and 1Z reaches more than 500 K (Figure S6). Single-crystal XRD reveals that 1E and 1Z have distinct crystallographic symmetry differences. 1Z adopts a centrosymmetric space group $P2_1/n$ (Table S1). The asymmetric unit of 1Z contains one molecule, and the dihedral angles between the benzene and the plane where the three oxygen atoms are located in succinic anhydride range from 43.5 to 46.4° (Figures 1a and S7). Interestingly, 1E

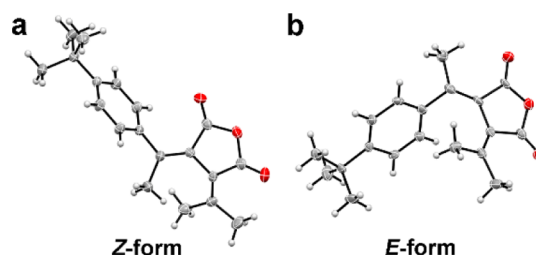


Figure 1. Molecular structures of 1Z (a) and 1E (b). The carbon, oxygen, and hydrogen atoms are labeled with gray, red, and white colors, respectively.

crystallizes in a monoclinic *Pc* space group, belonging to a non-centrosymmetric point group C_s , which was also confirmed by the second harmonic generation (SHG) result showing active intensity response (Figure S8). The asymmetric unit of 1E consists of four molecules, in which the dihedral angles mentioned above are 77.5 and 77.9° (Figures 1b and S7). More details of these crystal data are listed in Table S1.

Fulgide derivatives generally demonstrate typical photochromic properties benefiting from the unique chromophores with extended conjugation undergoing molecular photoisomerization behavior between ring-opening and ring-closing states.²⁹ Unfortunately, the photoreaction conversion of the fulgides in the solid state is generally insufficient to isolate the pure ring-closing production, thereby the crystal structures of 1Z and 1E are still going to be ring-opening form with almost the same crystallographic parameters before and after steady UV light irradiation (Table S1).⁵¹ Photoreaction mainly occurs at the solid sample surface but not in the core because UV light can hardly penetrate the bulk of the crystals. This commonly happens in the case of other photochromic salicylideneaniline Schiff base ferroelectrics.^{35–38} As shown in Figure 2a (inset), the color of 1E and 1Z shows reversible changes between

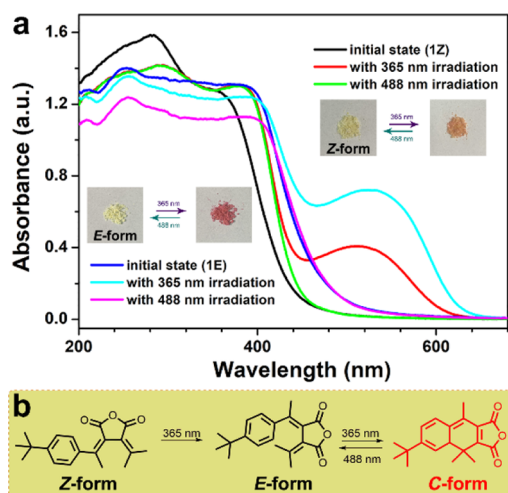


Figure 2. (a) UV–vis absorption spectra of 1E and 1Z before and after light irradiation, inset: photochromic images of 1E and 1Z. (b) Photoreaction path of fulgide in this work.

yellow and red under 365 and 488 nm light irradiation. The photochromism phenomenon was then recorded by solid-state UV–vis absorption spectra. Polycrystalline powder of 1Z and 1E exhibits absorption edges at 470 and 440 nm, respectively, assigned to the ring-opening forms. After being subjected to 365 nm UV light irradiation for the 60 s, new broad absorption bands emerge at around 525 nm. The peak intensity of 1E is stronger than that of 1Z, indicating a relatively faster transformation of 1E to 1C (ring-closing form) in this period. Upon the visible lighting, 1E shows the absorption edge that perfectly overlaps with the initial state. However, photoexcited 1Z does not go back to its initial state upon 488 nm light irradiation and demonstrates a light absorption spectrum similar to that of 1E. The intriguing phenomenon may be attributed to the more stable structure of 1E. Therefore, the photochromism is following the changes in the UV–vis absorption spectra on account of the photochemical conversion of the ring-opening form to the ring-closing form (Figure 2b). Time-dependent solid-state UV–vis spectra of the polycrystalline sample of 1E were also performed. As shown in Figure S9, the new absorption band around 525 nm gradually becomes saturated within the 60 s under the 365 nm UV light irradiation, suggesting that the photoreaction in the surface of the solid sample is basically completed. Subsequently, this absorption band decreases very quickly and completely vanishes within the 2 s upon further 488 nm visible light irradiation.

To further denote the situation of Z to E configuration transformation by light, dynamic tracking of NMR spectra by time was performed on 1Z in CDCl_3 under light irradiation. As recorded in Figure 3, with the increase of light irradiation time, the ^1H NMR spectra change significantly. Specifically, some chemical shift characteristic peaks ascribed to the Z-form have apparently weakened and disappeared, accompanied by the appearance of new peaks belonging to the E-form, marked with asterisks. In terms of light irradiation time, when the Z-form is exposed to light for 1 min, the E-form can be obviously detected by the NMR spectra. With the gradual increase of the exposure time to 6 min, it can be observed that the E- and Z-forms almost reach the same proportion. After 20 min of illumination, the proportion of the E-form has exceeded that of the Z-form. As the light irradiation time continues to increase,

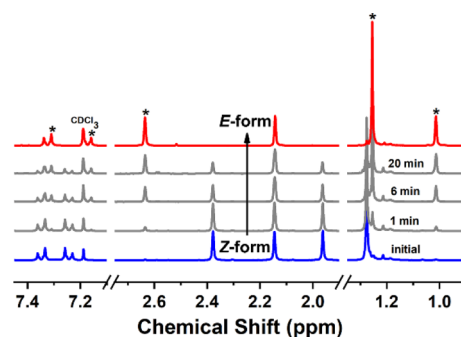


Figure 3. Configuration transformation from Z-form to E-form with light irradiation detected by ^1H NMR spectra. The asterisk indicates the appearance of the characteristic peaks corresponding to the E-form.

the NMR spectra did not change significantly, indicating that the transformation from Z to E reached an equilibrium state. In this process, we can gradually achieve complete conversion of the E-form through continuous column chromatography separation. The results are in good agreement with those of solid UV–vis spectra.

We also calculated the relative energy of each state of the 1Z, 1E, and 1C molecules to have a deeper understanding of the state changes before and after light irradiation. In Figure 4, the

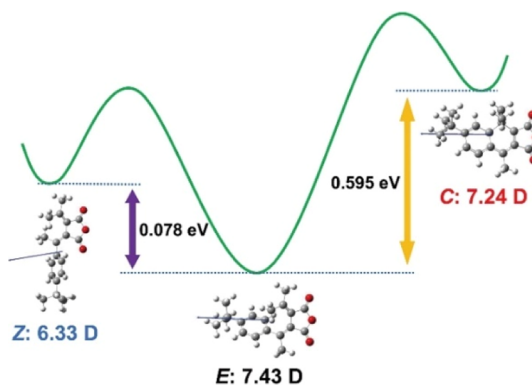


Figure 4. Energy and dipole evolution in the transformation process of ring-opening Z- and E-forms and the ring-closing C-form.

most stable state is the E-form, as indicated by the energy minimum state. Even the Z-form is 0.078 eV higher than the E-form. Among the three states, the ring-closed form 1C adopts the highest state, which is the most unstable. Compared with the E-form, the transformation upon light-irradiation from the Z-form to the ring-closed form can be described as two steps, first undergoing the Z-form to the E-form and then experiencing the E-form to the C-form. Experimentally, such two-step transformation is reflected by the relatively long conversion time and low conversion efficiency. In the subsequent ring-opening process, the final product is mostly the E-form structure, which is more stable than the Z-form. This speculation is consistent with the experimental UV–vis spectrum. In addition, the ring-opening and closing process of the E-form does not have a great influence on the modulus and direction of the molecular dipole. In contrast, the dipole moment changes obviously in the process from the Z-form to the C-form. The highest occupied molecular orbital (HOMO) and lowest unoccupied molecular orbital (LUMO) of 1Z, 1E, and 1C molecules were calculated (Figure S10), showing that

the electron density is distributed on the whole molecule. Between 1Z and 1E, the distribution and phase of HOMO and LUMO hardly changed, indicating that the electronic state between the Z- and the E-forms is very close. When 1E transforms into 1C, the molecular orbital changes significantly since such a process involves the rearrangement of electrons and the formation of new bonds.

The measurement of the polarization–voltage (P – V) hysteresis loop by the double-wave method was carried out on the 1E, which has a non-centrosymmetric ferroelectric point group. As demonstrated in Figure 5, distinct displacement

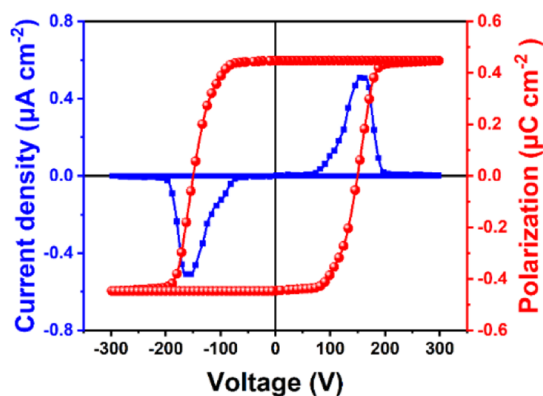


Figure 5. P – V hysteresis loop of 1E measured at room temperature.

current peaks are observed in 1E, and a well-opened P – V loop with the saturation polarization (P_s) value of $0.45 \mu\text{C}/\text{cm}^2$ was

recorded, strongly confirming the ferroelectricity of 1E. The ferroelectric hysteresis loop of 1E was also evaluated under the 365 nm UV light. However, no significant difference is observed between the measured macroscopic hysteresis loops before and after light irradiation. Probably, the main reason is ascribed to a similar total polarization of the E-form and the C-form (Figure 4). Besides, the low photoisomerization conversion of the fulgide bulk crystal may also lead to less difference for their ferroelectric loops. Similar situations have been found in previously reported photoswitchable salicylideneaniline Schiff base ferroelectric crystals.^{35–38} The intensity of the SHG signal for polycrystalline powder of 1E was recorded showing slight and reversible changes before and after light irradiation (Figure S11), which should correlate with the structural photoisomerization between the initial and excited states. PFM is a surface technique based on scanning probe microscopy. An a.c. voltage is applied through a conductive tip, causing piezo-response of the ferroelectric sample due to the converse piezoelectric effect. According to the amplitude and phase of the piezo-response, polarization distribution and domain structures can be derived. For this reason, we carried out PFM measurements to characterize the veritable ferroelectric polarization reversal at a microscopic level. Although the photochromic bulk crystals generally achieve a low photoreaction yield subject to the hard penetration of light into the crystals, the photoisomerization conversion on the surface of the thin film is relatively high. Therefore, PFM based on the surface technology is preferred to track and detect the ferroelectric polarization change by light.

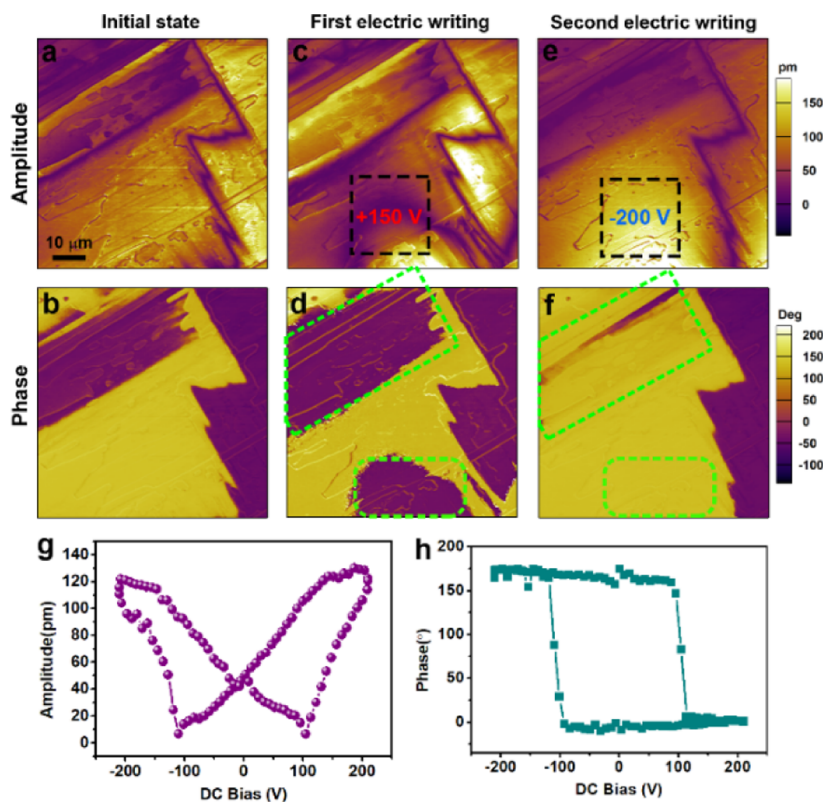


Figure 6. Polarization switching for the thin film of 1E by electric field. Out-of-plane PFM amplitude images (up row) and PFM phase images (middle row) of the selected region at the initial state (a,b), after applying tip voltage of +150 V on the region marked by the black box (c,d) and after applying tip voltage of -200 V on the same region (e,f). Local PFM amplitude butterfly (g) and phase hysteresis (h) loops on an arbitrary point of the 1E thin film.

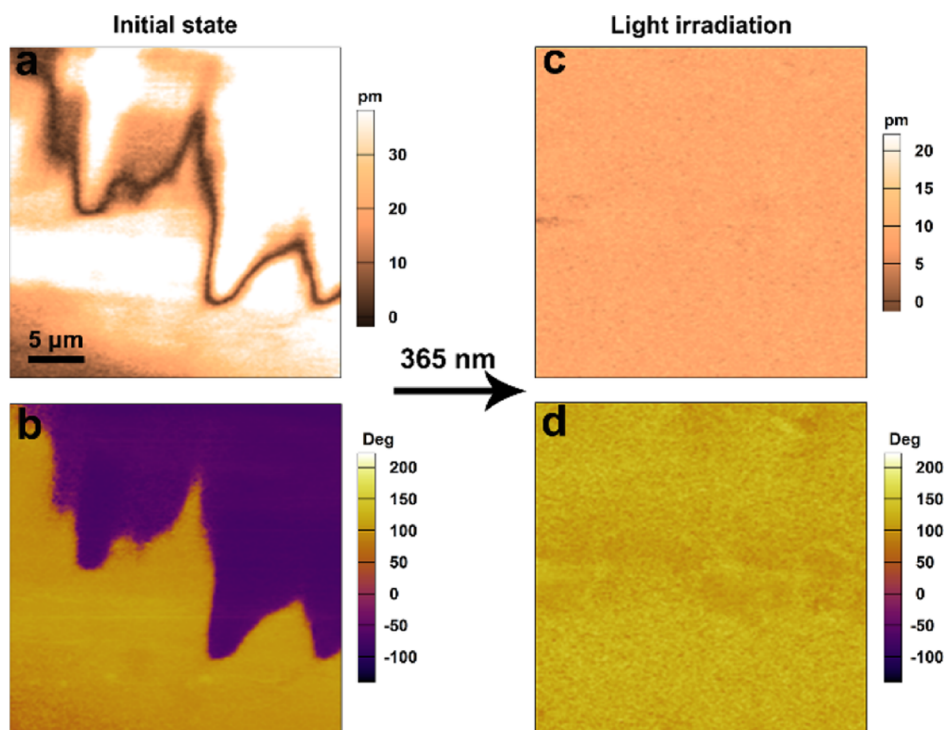


Figure 7. Light-induced manipulation of ferroelectric domains in the thin film of 1E. PFM amplitude (top row), PFM phase (middle row) images at the initial state (a,b) and light irradiation (c,d).

We carried out the domain switching measurements on the thin film of 1E. Figure 6a,b shows the out-of-plane PFM amplitude and phase images of the initial domain structure in the selected region, respectively. There are two types of domains in this region whose walls can be clearly discerned in the amplitude image, and they appear in the phase image as yellow and purple contrasts with a phase difference of $\sim 180^\circ$, respectively. We then apply a DC voltage of +150 V by PFM tip scanning in the relatively middle region of the yellow domain, as marked by the black box shown in Figure 6c. The subsequent PFM imaging is shown in Figure 6c,d. Near the region where the electric field was applied, a new domain with opposite phase contrast (purple) was generated, as marked by the green round rectangle in Figure 6d. Meanwhile, the purple domain in the upper left corner expands at the expense of the neighboring yellow domain under this positive electric field, as marked by a green dashed trapezium. This indicates that the yellow domain switches to the purple domain under the action of an electric field, that is, the polarization reversal occurs. In this process, polarization switching occurs in two ways: new domain nucleation and growth in the round rectangle region and the motion of the existing domain walls in the trapezoidal region. We further apply a larger opposite voltage of -200 V to the same region. We found that the new purple domain in the round rectangle region disappeared, and the purple domain in the upper left corner contracted, indicating that the polarization switched back under the action of the opposite electric field (Figure 6e,f). Moreover, we performed PFM spectroscopy on a single point of the thin film to study polarization switching and the local piezoresponse as a function of the DC tip bias. A well-defined off-field butterfly-shaped amplitude loop and a hysteretic phase loop verify the robust ferroelectricity in 1E (Figure 6g,h).

Moreover, light as an external field was also used to manipulate the ferroelectric polarization in the thin film of 1E. Figure 7a,b shows mappings of PFM amplitude and phase measured in the dark, while Figure 7c,d points to the corresponding mappings after 365 nm UV irradiation in the same region. The initial state exhibits a clear ferroelectric domain pattern with a clear domain wall. When the thin film was exposed to 365 nm UV light, the PFM scanning was repeated in the same area. It is observed that the purple domains in Figure 7b switch to yellow ones after 365 nm UV light irradiation. Besides, the disappearance and appearance of ferroelectric domains by lights have been evaluated. The as-grown domain structures of the thin film of the *E*-form are shown in Figure S12a,b, which were selected for the initial state. The PFM images were recorded for the same region as a function of the photoirradiation time. After 365 nm UV light irradiation for 20 min, the partial purple domains switch to the yellow ones (Figure S12c,d). As the irradiation time continuously increases to 60 min, the purple domains almost fully change to the yellow, as illustrated in Figure S12e–h. Upon the steadily visible 488 nm light irradiation for 6 h, we found that only some of the yellow domains switch back to purple (Figure S12i,j). The experimental results have clearly indicated the disappearance and appearance of ferroelectric domains by optical manipulation. The photo-triggered ferroelectric domain changes in the 1E thin film suggest a strong interaction between light and ferroelectric polarization. The photoisomerization produces a minor difference in polarization between ring-opening and ring-closing forms. The different polarization states can be manifested as the change in ferroelectric domains before and after light irradiation. Therefore, light can activate the reversible molecular conformational transformation of photochromic ferroelectrics and also trigger the manipulation of ferroelectric polarization.

In addition, we also notice that the formation and evolution of ferroelectric domains of fulgide crystal should be a very slow process. A similar situation has been found in the recently reported photoswitchable salicylideneaniline Schiff base ferroelectric system.³⁵

For application prospects, it is desirable for the matter to show good stability of physical properties. As to the 1E, the reproducibility of the photocyclization reaction is particularly important to its photo-triggered ferroelectricity. We herein performed the switching cycles of UV–vis spectra under light irradiation on 1E in the solid state and recorded the pattern changes of the absorbance band at 525 nm. As shown in Figure 8, 1E was repeatedly irradiated under 365 and 488 nm lights

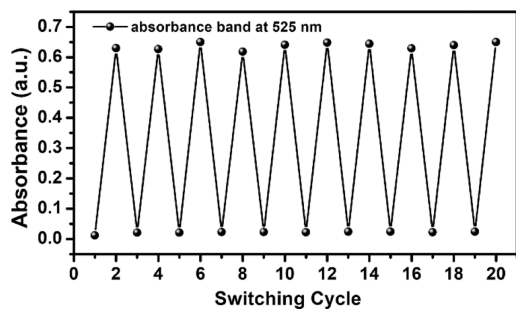


Figure 8. Absorbance band changes at 525 nm with repeated illumination of 365 and 488 nm lights, showing 1E a good fatigue resistance to photoirradiation.

for the 60 and the 2 s, respectively, at least 20 times without showing a significant change in the absorbance band intensity. The results reveal a very good fatigue resistance to photoirradiation and provide a future expectation for the fast optical control of ferroelectric switching devices.

CONCLUSIONS

In summary, we report the first photochromic organic fulgide ferroelectric showing an interesting photo-triggered polarization response. In the synthesis of new fulgide isomers, we successfully isolated the *E*- and *Z*-forms and characterized their crystal structures, photochromism, and ferroelectric properties, respectively. They have two completely different crystal structure symmetries that the 1E adopts a non-centrosymmetric *Pc* space group, while 1Z crystallizes in a centrosymmetric space group *P2₁/n*. Both the two fulgide isomers exhibit prominent photochromic behavior. The intriguing phenomenon is that the *Z*-form can be transformed into the *E*-form by light irradiation. The underlying mechanism has been revealed by spectral and computational data. Significantly, 1E with a non-centrosymmetric feature was verified with solid ferroelectricity by the electric field-controlled measurements of the *P*–*V* hysteresis loop and PFM ferroelectric domain switching. The ferroelectricity in fulgides has been rarely reported before. More interestingly, 1E presents prominent photo-triggered ferroelectric polarization response, being attributed to the pericyclic photoisomerization by light irradiation. This finding expands the application potential of fulgide derivatives for the optical control of ferroelectrics.

EXPERIMENTAL SECTION

Materials

Diethyl succinate (Aladdin 98%), diethyl isopropylidene succinate (Macklin 98%), 4-*tert*-butylacetophenone (Aladdin 98%), and sodium hydride (Macklin, 60% dispersion in mineral oil) were used. All conventional reagents and solvents were purchased and used without further purification. The synthesis details are described in the Supporting Information.

Measurements

Methods of single-crystal XRD, PXRD, UV–vis spectra, thin-film preparation, ferroelectric loop, PFM, and calculations are described in the Supporting Information.

ASSOCIATED CONTENT

Supporting Information

The Supporting Information is available free of charge at <https://pubs.acs.org/doi/10.1021/jacsau.3c00118>.

Detailed information regarding the synthesis and experimental methods (PDF)

Crystallographic data of 1E (CIF)

Crystallographic data of 1E under 365 nm irradiation (CIF)

Crystallographic data of 1Z (CIF)

Crystallographic data of 1Z under 365 nm irradiation (CIF)

Accession Codes

CCDC 2121133–2121136 contain the supplementary crystallographic data for this paper. These data can be obtained free of charge via www.ccdc.cam.ac.uk/data_request/cif.

AUTHOR INFORMATION

Corresponding Authors

Ren-Gen Xiong – Ordered Matter Science Research Center, Nanchang University, Nanchang 330031, People's Republic of China; orcid.org/0000-0003-2364-0193;
Email: xiongrg@seu.edu.cn

Zhong-Xia Wang – College of Chemistry and Chemical Engineering, Gannan Normal University, Ganzhou 341000, People's Republic of China; Ordered Matter Science Research Center, Nanchang University, Nanchang 330031, People's Republic of China; orcid.org/0000-0002-9012-5653;
Email: zhongxiawang@ncu.edu.cn

Authors

Ye Du – College of Chemistry and Chemical Engineering, Gannan Normal University, Ganzhou 341000, People's Republic of China

Chao-Ran Huang – College of Chemistry and Chemical Engineering, Gannan Normal University, Ganzhou 341000, People's Republic of China

Zhe-Kun Xu – Ordered Matter Science Research Center, Nanchang University, Nanchang 330031, People's Republic of China

Wei Hu – Ordered Matter Science Research Center, Nanchang University, Nanchang 330031, People's Republic of China

Peng-Fei Li – Ordered Matter Science Research Center, Nanchang University, Nanchang 330031, People's Republic of China

Complete contact information is available at: <https://pubs.acs.org/10.1021/jacsau.3c00118>

Author Contributions

The manuscript was written through contributions of all authors. CRediT: **Ye Du** data curation, investigation; **Chao-Ran Huang** data curation, investigation; **Zhe-Kun Xu** data curation; **Wei Hu** data curation; **Peng-Fei Li** data curation, software; **Ren-Gen Xiong** writing-review & editing; **Zhong-Xia Wang** conceptualization, writing-original draft, writing-review & editing.

Notes

The authors declare no competing financial interest.

ACKNOWLEDGMENTS

This work was supported by the National Natural Science Foundation of China (22222502 and 21991142).

REFERENCES

- (1) Irie, M.; Fukaminato, T.; Matsuda, K.; Kobatake, S. Photochromism of Diarylethene Molecules and Crystals: Memories, Switches, and Actuators. *Chem. Rev.* **2014**, *114*, 12174–12277.
- (2) Raymo, F. M.; Tomasulo, M. Electron and energy transfer modulation with photochromic switches. *Chem. Soc. Rev.* **2005**, *34*, 327–336.
- (3) Tian, H.; Yang, S. Recent progresses on diarylethene based photochromic switches. *Chem. Soc. Rev.* **2004**, *33*, 85–97.
- (4) Sendler, T.; Luka-Guth, K.; Wieser, M.; LokamaniWolf, J.; Wolf, J.; Helm, M.; Gemming, S.; Kerbusch, J.; Scheer, E.; Huhn, T.; et al. Light-Induced Switching of Tunable Single-Molecule Junctions. *Adv. Sci.* **2015**, *2*, 1500017.
- (5) Kobatake, S.; Takami, S.; Muto, H.; Ishikawa, T.; Irie, M. Rapid and reversible shape changes of molecular crystals on photo-irradiation. *Nature* **2007**, *446*, 778–781.
- (6) Bléger, D.; Hecht, S. Visible-Light-Activated Molecular Switches. *Angew. Chem., Int. Ed.* **2015**, *54*, 11338–11349.
- (7) Gao, Z.; Wang, K.; Yan, Y.; Yao, J.; Zhao, Y. S. Smart responsive organic microlasers with multiple emission states for high-security optical encryption. *Natl. Sci. Rev.* **2021**, *8*, nwaal62.
- (8) Du, Z.; Zhang, T.; Gai, H.; Sheng, L.; Guan, Y.; Wang, X.; Qin, T.; Li, M.; Wang, S.; Zhang, Y.-M.; Nie, H.; Zhang, S. X.-A. Multi-Component Collaborative Step-by-Step Coloring Strategy to Achieve High-Performance Light-Responsive Color-Switching. *Adv. Sci.* **2022**, *9*, 2103309.
- (9) Dong, H.; Zhu, H.; Meng, Q.; Gong, X.; Hu, W. Organic photoresponse materials and devices. *Chem. Soc. Rev.* **2012**, *41*, 1754–1808.
- (10) Wong, C.-L.; Ng, M.; Hong, E. Y.-H.; Wong, Y.-C.; Chan, M.-Y.; Yam, V. W.-W. Photoresponsive Dithienylethene-Containing Tris(8-hydroxyquinolino)aluminum(III) Complexes with Photo-controllable Electron-Transporting Properties for Solution-Processable Optical and Organic Resistive Memory Devices. *J. Am. Chem. Soc.* **2020**, *142*, 12193–12206.
- (11) Lines, M. E.; Glass, A. M. *Principles and Applications of Ferroelectrics and Related Materials*; Oxford University Press, 2001, pp 1–672.
- (12) Scott, J. F. Applications of Modern Ferroelectrics. *Science* **2007**, *315*, 954–959.
- (13) Ren, Y.; Wu, M.; Liu, J.-M. Ultra-high piezoelectric coefficients and strain-sensitive Curie temperature in hydrogen-bonded systems. *Natl. Sci. Rev.* **2021**, *8*, nwaal203.
- (14) Qiu, C.; Wang, B.; Zhang, N.; Zhang, S.; Liu, J.; Walker, D.; Wang, Y.; Tian, H.; Shrout, T. R.; Xu, Z.; et al. Transparent ferroelectric crystals with ultrahigh piezoelectricity. *Nature* **2020**, *577*, 350–354.
- (15) Wu, J.; Xiao, D.; Zhu, J. Potassium–Sodium Niobate Lead-Free Piezoelectric Materials: Past, Present, and Future of Phase Boundaries. *Chem. Rev.* **2015**, *115*, 2559–2595.
- (16) Valasek, J. Piezo-Electric and Allied Phenomena in Rochelle Salt. *Phys. Rev.* **1921**, *17*, 475–481.
- (17) Huang, C.-R.; Luo, X.; Chen, X.-G.; Song, X.-J.; Zhang, Z.-X.; Xiong, R.-G. A multiaxial lead-free two-dimensional organic-inorganic perovskite ferroelectric. *Natl. Sci. Rev.* **2021**, *8*, nwaal232.
- (18) Liu, H.-Y.; Zhang, H.-Y.; Chen, X.-G.; Xiong, R.-G. Molecular Design Principles for Ferroelectrics: Ferroelectrochemistry. *J. Am. Chem. Soc.* **2020**, *142*, 15205–15218.
- (19) Harada, J.; Shimojo, T.; Oyamaguchi, H.; Hasegawa, H.; Takahashi, Y.; Satomi, K.; Suzuki, Y.; Kawamata, J.; Inabe, T. Directionally tunable and mechanically deformable ferroelectric crystals from rotating polar globular ionic molecules. *Nat. Chem.* **2016**, *8*, 946–952.
- (20) Horiuchi, S.; Tokunaga, Y.; Giovannetti, G.; Picozzi, S.; Itoh, H.; Shimano, R.; Kumai, R.; Tokura, Y. Above-room-temperature ferroelectricity in a single-component molecular crystal. *Nature* **2010**, *463*, 789–792.
- (21) Shi, P.-P.; Tang, Y.-Y.; Li, P.-F.; Liao, W.-Q.; Wang, Z.-X.; Ye, Q.; Xiong, R.-G. Symmetry breaking in molecular ferroelectrics. *Chem. Soc. Rev.* **2016**, *45*, 3811–3827.
- (22) Wang, Z.-M.; Gao, S. Can molecular ferroelectrics challenge pure inorganic ones? *Natl. Sci. Rev.* **2014**, *1*, 25–26.
- (23) Xu, W.-J.; Romanyuk, K.; Martinho, J. M. G.; Zeng, Y.; Zhang, X. W.; Ushakov, A.; Shur, V.; Zhang, W. X.; Chen, X. M.; Kholkin, A.; et al. Photoresponsive Organic–Inorganic Hybrid Ferroelectric Designed at the Molecular Level. *J. Am. Chem. Soc.* **2020**, *142*, 16990–16998.
- (24) Morita, H.; Tsunashima, R.; Nishihara, S.; Inoue, K.; Omura, Y.; Suzuki, Y.; Kawamata, J.; Hoshino, N.; Akutagawa, T.; Akutagawa, T. Ferroelectric Behavior of a Hexamethylenetetramine-Based Molecular Perovskite Structure. *Angew. Chem., Int. Ed.* **2019**, *58*, 9184–9187.
- (25) Peng, Y.; Bie, J.; Liu, X.; Li, L.; Chen, S.; Fa, W.; Wang, S.; Sun, Z.; Luo, J. Acquiring High- T_C Layered Metal Halide Ferroelectrics via Cage-Confined Ethylamine Rotators. *Angew. Chem., Int. Ed.* **2021**, *60*, 2839–2843.
- (26) Liu, Y.; Han, S.; Wang, J.; Ma, Y.; Guo, W.; Huang, X.-Y.; Luo, J.-H.; Hong, M.; Sun, Z. Spacer Cation Alloying of a Homoconformational Carboxylate trans Isomer to Boost in-Plane Ferroelectricity in a 2D Hybrid Perovskite. *J. Am. Chem. Soc.* **2021**, *143*, 2130–2137.
- (27) Szafranski, M.; Katrusiak, A.; McIntyre, G. J. Ferroelectric Order of Parallel Bistable Hydrogen Bonds. *Phys. Rev. Lett.* **2002**, *89*, 215507.
- (28) Owczarek, M.; Hujsak, K.; Ferris, D. P.; Prokofjevs, A.; Majerz, I.; Szklarz, P.; Zhang, H.; Sarjeant, A. A.; Stern, C. L.; Jakubas, R.; Hong, S.; et al. Flexible ferroelectric organic crystals. *Nat. Commun.* **2016**, *7*, 13108.
- (29) Bisoyi, H. K.; Li, Q. Light-Driven Liquid Crystalline Materials: From Photo-Induced Phase Transitions and Property Modulations to Applications. *Chem. Rev.* **2016**, *116*, 15089–15166.
- (30) Vats, G.; Bai, Y.; Zhang, D.; Juuti, J.; Seidel, J. Optical Control of Ferroelectric Domains: Nanoscale Insight into Macroscopic Observations. *Adv. Opt. Mater.* **2019**, *7*, 1800858.
- (31) Rubio-Marcos, F.; Del Campo, A.; Marchet, P.; Fernández, J. F. Ferroelectric domain wall motion induced by polarized light. *Nat. Commun.* **2015**, *6*, 6594.
- (32) Jiang, J.; Bai, Z. L.; Chen, Z. H.; He, L.; Zhang, D. W.; Zhang, Q. H.; Shi, J. A.; Park, M. H.; Scott, J. F.; Hwang, C. S.; et al. Temporary formation of highly conducting domain walls for non-destructive read-out of ferroelectric domain-wall resistance switching memories. *Nat. Mater.* **2018**, *17*, 49–56.
- (33) Nova, T. F.; Disa, A. S.; Fechner, M.; Cavalleri, A. Metastable ferroelectricity in optically strained SrTiO₃. *Science* **2019**, *364*, 1075–1079.
- (34) Tang, Y.-Y.; Zeng, Y.-L.; Xiong, R.-G. Contactless Manipulation of Write–Read–Erase Data Storage in Diarylethene Ferroelectric Crystals. *J. Am. Chem. Soc.* **2022**, *144*, 8633–8640.
- (35) Tang, Y.-Y.; Liu, J.-C.; Zeng, Y.-L.; Peng, H.; Huang, X.-Q.; Yang, M.-J.; Xiong, R.-G. Optical Control of Polarization Switching in

a Single-Component Organic Ferroelectric Crystal. *J. Am. Chem. Soc.* **2021**, *143*, 13816–13823.

(36) Wang, Z.-X.; Chen, X.-G.; Song, X.-J.; Zeng, Y.-L.; Li, P.-F.; Tang, Y.-Y.; Liao, W.-Q.; Xiong, R. G. Domain memory effect in the organic ferroics. *Nat. Commun.* **2022**, *13*, 2379.

(37) Liao, W.-Q.; Zeng, Y.-L.; Tang, Y.-Y.; Peng, H.; Liu, J.-C.; Xiong, R.-G. Multichannel Control of Multiferroicity in Single-Component Homochiral Organic Crystals. *J. Am. Chem. Soc.* **2021**, *143*, 21685–21693.

(38) Liao, W. Q.; Deng, B. B.; Wang, Z. X.; Cheng, T. T.; Hu, Y. T.; Cheng, S. P.; Xiong, R. G. Optically Induced Ferroelectric Polarization Switching in a Molecular Ferroelectric with Reversible Photoisomerization. *Adv. Sci.* **2021**, *8*, 2102614.

(39) Yokoyama, Y. Fulgides for Memories and Switches. *Chem. Rev.* **2000**, *100*, 1717–1740.

(40) Heller, H. G.; Oliver, S. Photochromic heterocyclic fulgides. Part 1. Rearrangement reactions of (*E*)- α -3-furylethylidene-(isopropylidene)succinic anhydride. *J. Chem. Soc. Perkin Trans. I* **1981**, *1*, 197–201.

(41) Fan, M.; Yu, L.; Zhao, W. Fulgide Family Compounds: Synthesis, Photochromism, and Applications. In *Organic Photochromic and Thermochromic Compounds*; Crano, J. C., Guglielmetti, R., Eds.; *Main Photochromic Families*; Plenum Publishers: New York, 1999; Vol. 1, Chapter 4, pp 141–206.

(42) Weerasekara, R. K.; Uekusa, H.; Hettiarachchi, C. V. Multicolor Photochromism of Fulgide Mixed Crystals with Enhanced Fatigue Resistance. *Cryst. Growth Des.* **2017**, *17*, 3040–3047.

(43) Reinfelds, M.; Hermanns, V.; Halbritter, T.; Wachtveitl, J.; Braun, M.; Slanina, T.; Heckel, A. A Robust, Broadly Absorbing Fulgide Derivative as a Universal Chemical Actinometer for the UV to NIR Region. *ChemPhotoChem* **2019**, *3*, 441–449.

(44) Janicki, S. Z.; Schuster, G. B. A Liquid Crystal Opto-optical Switch: Nondestructive Information Retrieval Based on a Photochromic Fulgide as Trigger. *J. Am. Chem. Soc.* **1995**, *117*, 8524–8527.

(45) Harada, J.; Taira, M.; Ogawa, K. Photochromism of Fulgide Crystals: From Lattice-Controlled Product Accumulation to Phase Separation. *Cryst. Growth Des.* **2017**, *17*, 2682–2687.

(46) Chen, Y.; Wang, C.; Fan, M.; Yao, B.; Menke, N. Photochromic fulgide for holographic recording. *Opt. Mater.* **2004**, *26*, 75–77.

(47) Eichler, C.; Rázková, A.; Müller, F.; Kopacka, H.; Huppertz, H.; Hofer, T. S.; Schwartz, H. A. Paving the Way to the First Functional Fulgide@MOF Hybrid Materials. *Chem. Mater.* **2021**, *33*, 3757–3766.

(48) Jiao, Y.; Yang, R.; Luo, Y.; Liu, L.; Xu, B.; Tian, W. Fulgide Derivative-Based Solid-State Reversible Fluorescent Switches for Advanced Optical Memory. *CCS Chem.* **2022**, *4*, 132–140.

(49) Liang, Y. C.; Dvornikov, A. S.; Rentzepis, P. M. Nonvolatile read-out molecular memory. *Proc. Natl. Acad. Sci. U.S.A.* **2003**, *100*, 8109–8112.

(50) Tomasello, G.; Bearpark, M. J.; Robb, M. A.; Orlandi, G.; Garavelli, M. Significance of a Zwitterionic State for Fulgide Photochromism: Implications for the Design of Mimics. *Angew. Chem., Int. Ed.* **2010**, *122*, 2975–2978.

(51) Harada, J.; Nakajima, R.; Ogawa, K. X-ray Diffraction Analysis of Photochromic Reaction of Fulgides: Crystalline State Reaction Induced by Two-Photon Excitation. *J. Am. Chem. Soc.* **2008**, *130*, 7085–7091.

(52) Dong, W. L.; Zhao, B. X.; Wei, F.; Zuo, H.; Shin, D. S. Unexpected Novel Rearrangement Reaction: Synthesis of Benzo-Medium-Ring Anhydride. *Synth. Commun.* **2008**, *38*, 1224–1235.